2020-03-03

Plastic CTOD as fatigue crack growth characterising parameter in 2024T3 and 7050T6 aluminium alloys using DIC

VascoOlmo, JM

10.1111/ffe.13210
Fatigue and Fracture of Engineering Materials and Structures
Wiley

Plastic CTOD as fatigue crack growth characterising parameter in 2024-T3 and 7050-T6 aluminium alloys using DIC

J.M. Vasco-Olmo[1*], F.A. Díaz[1], F.V. Antunes[2], M.N. James[3, 4]

[1] Departamento de Ingeniería Mecánica y Minera, University of Jaén, Jaén, Spain.

[2] Department of Mechanical Engineering, University of Coimbra, Coimbra, Portugal.

[3] School of Engineering, University of Plymouth, Plymouth, United Kingdom.

[4] Department of Mechanical Engineering, Nelson Mandela Metropolitan University, Port Elisabeth, South Africa.

*corresponding author: jvasco@ujaen.es

Abstract. The plastic range of crack tip opening displacement (CTOD) has been used for the experimental characterisation of fatigue crack growth for 2024-T3 and 7050-T6 aluminium alloys by using digital image correlation (DIC). The analysis of a full loading cycle allowed resolving the CTOD into elastic and plastic components. Fatigue tests were conducted on compact-tension (CT) specimens with a thickness of 1 mm and a width of 20 mm at different stress ratios (0.1, 0.3 and 0.5). The range of the plastic CTOD could be related linearly to *da/dN* independent of stress ratio for both alloys. To allow accurate measurements of CTOD, a method was obtained for correctly locating the crack tip and to explore the effect of the measurement position behind the crack tip, a sensitivity analysis was performed. The plastic range of CTOD has been demonstrated to be a suitable and alternate parameter to the stress intensity factor range for characterising fatigue crack propagation. A particularly innovative aspect is that the paper describes a DIC-based technique that the authors believe gives a reliable way to find the appropriate point to measure CTOD.

Keywords. CTOD, fatigue crack growth, DIC, 2024-T3 and 7050-T6 aluminium alloys.

Nomenclature:

a:	crack length
CJP:	crack tip fields model developed by Christopher, James and Patterson
COD:	crack opening displacement
CT:	compact tension specimen
CTOD:	crack tip opening displacement
$CTOD_{el}$:	elastic component of crack tip opening displacement
$CTOD_p$:	plastic component of crack tip opening displacement
$CTOD_t$:	total crack tip opening displacement
da/dN:	crack growth rate per cycle
DIC:	digital image correlation technique
E:	Young's modulus
L_x:	distance in the parallel direction to the crack for the CTOD measurement
L_y:	distance in the perpendicular direction to the crack plane for the CTOD measurement
MT:	middle tension specimen
P:	load
R:	ratio between the minimum and maximum load
W:	width of the specimen
ΔCOD:	range of crack opening displacement
ΔCTOD:	range of crack tip opening displacement
$\Delta CTOD_{el}$:	range of elastic crack tip opening displacement
$\Delta CTOD_p$:	range of plastic crack tip opening displacement
ΔJ:	range of J integral
ΔK:	range of stress intensity factor
v:	Poisson's ratio of the material
σ_{ys}:	yield stress of the material

1. Introduction

Although composite materials are currently being extensively used in modern commercial aircraft, aluminium alloys (AA) remain the materials of choice for the airframe in most commercial aircrafts. Among them, AA2024-T3 and AA7050-T6 are particularly relevant to the aerospace industry due to their low density, high strength and good resistance to fatigue crack propagation and corrosion[1]. As will be discussed below, the concept of characterising fatigue crack growth rate using CTOD has been the subject of significant research, but the utility of DIC measurements to obtain the plastic range of CTOD ($\Delta CTOD_p$) is still somewhat controversial. The present authors have previously presented a preliminary study of fatigue crack growth in commercially pure titanium and identified a 2D DIC technique that allows accurate identification of the plastic range of CTOD[2]. A linear relationship was observed between crack propagation rate (da/dN) and $\Delta CTOD_p$. This work extends the technique to the characterisation of fatigue crack propagation in two aluminium alloys commonly used in aircraft industrial applications.

The stress intensity factor range (ΔK) has traditionally been used as a characterising parameter for fatigue crack growth in applications subjected to small-scale yielding. In this respect, the Paris relationship[3,4] has been extensively applied for characterising crack propagation rate. However, this relationship has some limitations[5,6]: (i) it is based on empirical observations and does not add understanding on the mechanisms driving fatigue crack growth, and the constant obtained from the fitting present physically unjustifiable units; (ii) it is only valid for (relatively) large cracks under small-scale yielding conditions subjected to constant amplitude loading cycle; and (iii) crack growth rate per cycle depends on other parameters such as applied load ratio and load history which can invalidate the similitude concept that underpins the limited validity of the power relationship Paris relationship.

These limitations reflect the fact that stress intensity factor is a parameter defined to describe linear elastic conditions at the crack tip while fatigue crack propagation is controlled by nonlinear plasticity processes at the crack tip. The two most frequently used parameters in elastic-plastic fracture mechanics are CTOD and the J contour integral[7]. While both parameters are applied to materials that exhibit elastic-plastic behaviour at the crack tip and can also be used as a fracture criterion, the J integral is a global nonlinear elastic parameter and hence can also suffer from plasticity-induced loss of similitude. CTOD is a local parameter used to measure the opening originated at the tip of a crack as the component is loaded that therefore takes account of crack tip plasticity, although defining the precise point behind the absolute crack tip where the

opening displacement should be characterised can also be problematic. CTOD is used in this work as the parameter for characterising fatigue crack growth and a DIC-based technique is described that the authors believe gives a reliable way to find the appropriate point to measure CTOD.

Since Wells[8] proposed CTOD in 1961, it has been extensively used for fatigue crack growth characterisation since it is a more mechanistically-based approach[6] than phenomenological Paris relationship. Using the slip-based blunting mechanism at the crack tip proposed by Laird and Smith[9] and Pelloux[10], McClintock[11] showed that crack growth advance could be related to ΔCTOD. A sharp crack extends through alternating shear and therefore becomes blunted. Crack propagation and striation formation on the fracture surface were caused by the successive blunting and re-sharpening originated at the crack tip during each loading cycle. Nicholls[12] explored the crack blunting concept and found for different alloys a polynomial relationship between crack opening and crack advance. Donahue et al.[13] reported that da/dN and COD could be related for many different materials by a constant of proportionality and the threshold stress intensity factor. Shahani et al.[14] proposed two potential relationships to relate da/dN to ΔCTOD and ΔJ where the constants remained unchanged with respect to stress ratio changes. Fatigue tests were conducted on steel compact tension (CT) specimens keeping constant the loading amplitude and applying stress ratio values between 0.33 and 0.6.

Fatigue crack growth rate has been also numerically modelled using CTOD as the characterising parameter. Gu and Ritchie[15] used a geometric crack tip blunting CTOD model to characterise crack advance without introducing any specific failure criterion or presumed slip behaviour. Reasonable agreement between the numerical results and experimental data of fatigue crack propagation rate was found for 7075-T6 aluminium alloy using a linear da/dN–ΔCTOD relationship. Tvergaard[16] extended the work by Gu and Ritchie by continuing the cyclic loading up to 200 cycles via re-meshing at different stages of the plastic deformation. It was shown that CTOD commonly underwent a temporary behaviour, without crack closure during several cycles, before a constant behaviour with closure effect started to gradually develop. In more recent numerical studies, Antunes and co-workers[5,17] have modelled fatigue crack propagation based on the plastic component of CTOD for three different aluminium alloys: 6016-T4, 6082-T6 and 7050-T6. Different da/dN–ΔCTODp relationships independent of R-ratio were found, polynomial[17] for 6016-T4 and 6082-T6 aluminium alloys and linear[5] for 7050-T6 aluminium alloy. From this work the authors concluded that CTOD could be an alternate parameter to ΔK in the fatigue crack growth characterisation.

The digital image correlation (DIC) technique has been widely applied to problems in experimental mechanics and analysis of structural integrity problems over the last 30 years[18,19]. However, relatively few studies have considered the experimental analysis of CTOD using DIC. Khor et al.[20] used the δ_5 method[21] with DIC to measure the CTOD, where δ_5 is the CTOD measurement from two points on the surface of the specimen initially set 5 mm apart. Their work used single edge notched bend (SENB) specimens of austenitic stainless steel and the results were compared with CTOD measurements obtained both from the silicon replication method and clip gauge fracture toughness measurements. The measured CTOD value therefore did not correspond to that originally defined by Wells[8] as the opening at the tip of a crack. Recently, Samadian et al.[22] have proposed a novel method for the CTOD measurement over the entire crack font by measuring three-dimensional profile of the notched surface with 3D DIC. This method was verified by measurements of silicone replicas in addition to the analysis by the finite element method. In addition to the work reported by these authors, just a couple of other studies (to the authors knowledge) have been reported in the literature. Ktari et al.[23] investigated fatigue crack propagation of AISI 4130 forged steel at loading ratios of 0.1 and 0.7. They proposed a 2D DIC approach based on ΔCTOD to characterise fatigue crack growth and concluded that ΔCTOD could be a viable characterising parameter for fatigue crack propagation. They measured ΔCTOD using two virtual displacement gauges that formed an extensometer that was positioned at various distances behind the crack tip, obtaining the value of ΔCTOD by extrapolating the results to $a = 0$. Recently, the authors of the present work[2] have used 2D DIC measurements of CTOD to explore its ability for characterising fatigue crack growth in commercially pure titanium. The results of this work showed that the plastic component of CTOD could be directly linked with plastic crack tip deformation during crack propagation leading to the conclusion that $\Delta CTOD_p$ was a suitable parameter to characterise fatigue crack propagation. A linear relationship independent of stress ratio was obtained between da/dN and $\Delta CTOD_p$ ($da/dN = 0.2706\ \Delta CTOD_p$). That work was intended as a preliminary study to determine whether DIC techniques could be applied with sufficient accuracy to measure sub-micron CTOD displacements, as some previous work[24] had questioned whether the accuracy of DIC was adequate to obtain conclusive data. A commercially pure titanium alloy was chosen for this preliminary study since previous work[25–27] had shown that the microstructure of this material is highly amenable to the use of DIC techniques and to subsequent analysis and interpretation of the data. Examples of such work include estimating both the size and shape of the crack tip plastic zone under constant[25] and variable[26] amplitude loadings, as well as calculation of the stress intensity factors defined by the CJP crack tip field

model[28] that accurately characterise the mechanisms driving a growing fatigue crack[27]. The current work extends this preliminary work to the more microstructurally complex aluminium alloys (2024-T3 and 7050-T6) of interest in aerospace and transport applications. Fatigue tests at *R*-ratios of 0.1, 0.3 and 0.5 were conducted on each alloy using CT specimens 1 mm thick and 20 mm in width (*W*). The work used the methodology proposed in[2] to locate the crack tip and to perform a sensitivity analysis to establish the position of the two points located behind the crack tip for the accurate CTOD measurement. The authors believe that this sensitivity analysis process unambiguously identifies the appropriate position behind the crack tip to measure CTOD and avoids inaccuracies from the use of approximate solutions.

2. Material and experimental methods

Table 1 presents mechanical property data for the AA2024-T3 and AA7050-T6 alloys obtained from tension tests. All CT specimens had dimensions in accordance with ASTM E647[29] as shown in Figure 1. Fatigue tests at stress ratio values of 0.1, 0.3 and 0.5 were performed applying a maximum load of 600 N.

The experimental set-up used in the lab to conduct the fatigue tests and data acquisition is shown in Figure 2a. A random black speckle (shown in Figure 2b) was sprayed with an airbrush over a white background on one surface of each specimen for DIC measurements. Fatigue tests used a 25 kN servohydraulic machine (MTS 370.02) and a load frequency of 10 Hz. For the correct implementation of 2D DIC, a CCD camera (AVT Stingray F-504 B/C) was placed perpendicularly to the specimen surface, increasing the spatial resolution around the crack tip by focusing with a zoom lens (MLH-10X EO). The camera system was arranged to visualise the crack propagation at the centre of the image (as seen in Figure 2b), getting a resolution of 8.8 μm/pixel (field of view of 14.1 x 10.6 mm). A fibre optic light source (Fiber-Lite DC-950) was used to illuminate the speckled surface of the specimen and to enable a better observation of the speckle pattern and improved image processing.

Image processing was performed using the Vic-2D program[30] from the Correlated Solutions Company with 25 pixels as the subset size and a step value of 1 pixel to obtain the maximum resolution for the displacement maps. Figure 3 shows an example of the displacement fields obtained for the 7050 aluminium alloy for a load of 600 N and a 9.13 mm crack.

3. Crack tip location

Since the CTOD was originally defined as the opening at the crack tip[8], a particularly important aspect in its measurement is ensuring accurate location of the crack tip, as this assumed location will have a strong influence in the consistency of the results. Hence the methodology outlined by the authors in a previous work for locating the crack tip[2] was applied. CTOD measurement was found from the vertical displacement maps by selecting a pair of points behind the crack tip to measure the relative displacement between the crack faces. The *x* and *y* coordinates of the crack tip were obtained as follows. Firstly, the *y*-coordinate is found as the intersection point observed when a set of vertical displacement profiles, perpendicularly plotted to the crack path, cross the crack plane. This convergent behaviour of the profiles at a point on the crack plane can be clearly seen in Figure 4a. In the example shown in Figure 4a, the range in the *x*-direction of the plotted profiles is between 710 and 740 pixels since it was established as potential location of the crack tip. The vertical displacement value (0.188 mm) corresponding to this intersection point is also shown in Figure 4a because it is used to locate the crack tip in the *x*-direction (Figure 4b). Figure 4b plots a vertical displacement profile in the *x*-direction parallel to the crack direction and allows identification of the *x*-coordinate of the crack tip as that point on the displacement profile that has the same value for the vertical displacement (v = 0.188 mm) than that located in the identification procedure of the *y*-coordinate of the crack tip. The *x* and *y* coordinates identified for the crack tip location from this procedure were 722 and 623 pixels, respectively, taking the upper left corner of the vertical displacement map (Figure 3b) as the coordinate origin. This methodology was applied for all the crack lengths measured during the fatigue testing.

4. Influence on CTOD measurement of the located position behind the crack tip

The location of the two points behind the crack tip used to measure the CTOD is a critical aspect in the interpretation of CTOD data and its subsequent application to fatigue crack propagation. For this reason, a sensitivity study to explore how the *x* and *y* positions used for the CTOD measurement can influence on its value. As shown in Figure 5, two distances behind the crack tip are used to define the CTOD measurement position, one parallel to the crack direction (defined as L_x) and other one perpendicular to the crack (defined as L_y).

The sensitivity analysis was performed by analysing the variation of the CTOD values obtained at the maximum load corresponding to a range of values for one of the measurement position distances, whilst keeping fixed the other one. CTOD profiles showing its variation with the L_x measurement distance for values of L_y from 1 pixel (8.8

μm) to 20 pixels (176 μm) are plotted in Figure 6a. As expected, in all cases there is a stable increase in CTOD values as the L_x distance increases. However, an interesting observation is that the displacement profiles as a function of L_y converge to a point once L_y > 15 pixels (= 132 μm), and this point corresponds to a value of L_x of 14 pixels (= 123.2 μm). This behaviour is shown in greater detail in Figure 6b, where only displacement profiles for values of L_y > 15 pixels (132 μm) have been plotted. This magnifies the region around the intersection point (marked with a square). Corresponding behaviour is also observed in Figure 6c, where displacement profiles are plotted as a function of the L_y measurement distance for a range of L_x between 1 pixel (8.8 μm) and 20 pixels (176 μm). It is observed how for L_x values ≥14 pixels (= 123.2 μm) the CTOD profile reaches a constant value at a L_y distance of 15 pixels (= 132 μm). The constant value region is marked with the rectangle in Figure 6c. This analysis shows that the CTOD is uniquely and exactly measured by employing data obtained from two points located behind the crack tip with L_x distance of 14 pixels (123.2 μm) and L_y distance of 15 pixels (132 μm). All CTOD measurements were therefore made a distance L_x = 123.2 μm behind the crack tip and a distance L_y = 132 μm from the crack plane.

5. Results and discussion

The results of the experimental measurements of elastic and plastic CTOD components are discussed and the plastic range of CTOD is shown to correlate fatigue crack growth rate data.

5.1. Experimental determination of plastic CTOD

CTOD can be resolved into its elastic and plastic components from analysis of a full loading cycle. Figure 7 shows a typical CTOD plot for a crack 9.13 mm long in a 7050-T6 aluminium specimen analysed at a stress ratio of 0.1. CTOD data is plotted at loading step of 20 N along a complete loading cycle. The analysis of the plot shown in Figure 7 allows obtaining the range of elastic and plastic CTOD, where the different behaviours observed during the load cycle have been identified using upper case letters. The loading part of the cycle between points *A* and *B* (60 N to 140 N) is associated with crack opening. Once the crack is open, there is a linear regime between points *B* and *C* (140 N and 320 N) which is attributed to the elastic behaviour. From point *C*, however, the curve becomes nonlinear until point *D* (maximum load, 600 N) which is linked to plastic deformation at the crack tip. The procedure followed to separate the CTOD into elastic and plastic components essentially requires extrapolating the linear regime between *B* and *C* to the point of maximum load (shown

in Figure 7). Considering the unloading half cycle, between points *D* and *E* the CTOD values linearly decreases with the same slope as that found between points *B* and *C* for the loading half cycle. As the load is decreased below point *E* there is a deviation from linearity due to the reversed plastic deformation.

The recommended practice in Appendix X2 of the ASTM E 647 standard[29], that deals with the determination of opening load from compliance, forms the basis of the procedure adopted in this work to obtain the elastic and plastic components of CTOD. This procedure determines the point where the change in the linearity from elastic behaviour occurs (point *C* in Figure 7). Firstly, starting just above the point marking the opening region (point *B* in Figure 7), a least squares straight line (line drawn in Figure 7) was fitted to a segment of the experimental data spanning a range of 25% of the load cycle. The slope of this straight line was taken to represent the slope of the part corresponding to the elastic deformation of the loading cycle. Subsequently, segments of the load cycle spanning a range of three data points (7.4% of the cyclic load range) and that overlapped each other by one data point (3.7% of the cyclic load range) were used to fit least-squares straight lines, and the slope of each segment was determined. This procedure is schematically shown in Figure 8a. Finally, the relative error in slope for each segment, compared with the elastic opening slope, was calculated and plotted as a function of the applied load (Figure 8b). The point corresponding with a transition between elastic and plastic behaviour was defined as that load value where the relative error is > 5%.

The methodology described above to determine the elastic and plastic ranges of CTOD was used to analyse the CTOD data from all the tests. Figure 9 presents the results obtained for both aluminium alloys for the ranges of elastic and plastic CTOD along crack length. The data for the elastic range of CTOD show significant scatter, while those corresponding to the plastic CTOD range show a less scattered and gradually increasing behaviour as the crack grows.

5.2. Experimental fatigue crack growth characterisation by plastic range of CTOD

Figure 10 presents crack growth rate plots as d*a*/d*N* versus total ($CTOD_t$), elastic ($CTOD_{el}$) and plastic ($CTOD_p$) CTOD range for the 2024-T3 alloy (Figure 10a) and the 7050-T6 alloy (Figure 10b). In both alloys, it is clearly observed that only the CTOD plastic range exhibits a linear increase with crack propagation rate and can be used therefore as a fatigue crack growth characterising parameter. Figure 11 shows the resulting d*a*/d*N*–$\Delta CTOD_p$ relationships for both alloys and there is a clear linear

relationship that is independent of stress ratio in each case. These growth rate equations are given below:

AA2024-T3: $$\frac{da}{dN} = 0.4982\Delta CTOD_p \quad (2)$$

AA7075-T6: $$\frac{da}{dN} = 0.7313\Delta CTOD_p \quad (3)$$

Several points should be noted about these relationships; firstly, these equations are linear rather than logarithmic, as is necessary when using the Paris relationship. Secondly, both d*a*/d*N* and $\Delta CTOD_p$ have units of length, and hence the slopes of the growth rate relationships in Equations (2) and (3) are dimensionless, in contrast with the constants defined by the Paris relationship. According to this, the constants in Equations (2) and (3) can be established as an intrinsic property of the material since they do not depend on stress ratio. Recently, Antunes et al.[5] have also reported a linear variation between experimental d*a*/d*N* data and numerical $\Delta CTOD_p$ data on MT specimens of 7050-T6 alloy. Their work combined numerical modelling of CTOD using a methodology they had proposed in earlier work[17], with experimental data of crack propagation rate obtained for different values of stress ratio. They found a different crack growth rate slope of 0.5246 compared with the value of 0.7313 obtained in the present work. This difference may have arisen either because of the difference in methods (reference 5 combines numerical modelling with experimental data while the present work is entirely experimental) or from the difference in specimen geometry. Whilst these aspects require further work to understand and resolve, the most important conclusion from both studies is that a linear relationship exists between crack advance per cycle and the plastic range of CTOD.

6. Conclusions

Fatigue crack propagation rate in both 2024-T3 and 7050-T6 aluminium alloys has been shown to have a linear relationship with the plastic range of CTOD. This work has demonstrated that it is experimentally possible using DIC to measure the elastic and plastic components of CTOD as the relative displacement between the crack flanks. This work has further shown that DIC techniques can be successfully used to measure sub-micron values of ΔCTODp in microstructurally complex aluminium alloys as well as in more equiaxed CP titanium[2]. A sensitivity analysis of measurement point location, both horizontally behind the crack tip and vertically from the crack plane, indicated that an optimum position exists for these measurements. The measurement location identified through the sensitivity analysis is believed to give the correct value of the blunting CTOD, based on the shape and motion of the various CTOD profiles (Figure

6). The data in Figure 6 indicate that the CTOD value was accurately measured by using two points located a distance behind the crack tip of 123.2 μm and a distance perpendicular to the crack plane of 132 μm. To obtain accurate measurements of CTOD the crack tip must be correctly located and this was done using the method reported by the present authors in a previous paper[2].

Finally, it is clear that the use of CTOD as a parameter to characterise fatigue crack propagation rate offers a more physically meaningful and mechanistically-based interpretation of fatigue crack growth rate than is possible with the stress intensity factor range defined by Paris. Since CTOD also considers crack shielding and fatigue threshold in an intrinsic way[5] it avoids several of the similitude problems associated with the use of the linear elastic ΔK parameter to describe non-linear plasticity-based fatigue crack growth.

Acknowledgements

The authors want to acknowledge the financial support from the Spanish Government through the research project “Proyecto de Investigación de Excelencia del Ministerio de Economía y Competitividad MAT2016-76951-1-P”, without which this work could not have been performed.

References

1. Williams JC and Starke EA Jr. Progress in structural materials for aerospace systems. *Acta Materiala*. 2003; 51: 5775–5799.
2. Vasco-Olmo JM, Díaz FA, Antunes FV, James MN. Characterisation of fatigue crack growth using digital image correlation measurements of plastic CTOD. *Theoretical and Applied Fracture Mechanics*. 2019; 101: 332–341.
3. Paris PC, Gomez MP, Anderson WE. A rational analytical theory of fatigue. *Trend Engineering*. 1961; 13: 9–14.
4. Paris PC, Erdogan F. A critical analysis of crack propagation laws. *Journal of Basic Engineering*. 1963; 85(4): 528–534.
5. Antunes FV, Branco R, Prates PA, Borrego L. Fatigue crack modelling based on CTOD for the 7050-T6 alloy. *Fatigue & Fracture of Engineering Materials & Structures*. 2017; 40: 1309–1320.
6. Hosseini ZS, Dadfarnia M, Somerday BP, Sofronis P, Ritchie RO. On the theoretical modelling of fatigue crack growth. *Journal of the Mechanics and Physics of Solids*. 2018; 121: 341–362.
7. Anderson TL. *Fracture Mechanics: Fundamentals and Applications*. Boca Raton, USA: CRC Press LLC; 2005.
8. Wells AA. Unstable crack propagation in metals-cleavage and fast fracture. *Proceedings of the Crack Propagation Symposium*. 1961; 1(84): Cranfield, UK.
9. Laird C, Smith GC. Crack propagation in high stress fatigue. *The Philosophical Magazine: A Journal of Theoretical Experimental and Applied Physics*. 1962; 7(77): 847–857.
10. Pelloux RMN. Crack extension by alternating shear. *Engineering Fracture Mechanics*. 1970; 1: 697–704.
11. McClintock FA. Discussion to C. Laird's paper 'the influence of metallurgical microstructure on the mechanisms of fatigue crack propagation'. In: *Fatigue Crack Propagation*, ASTM STP 415. 1967; American Society for Testing and Materials, Philadelphia, PA: 170–174.
12. Nicholls DJ. The relation between crack blunting and fatigue crack growth rates. *Fatigue & Fracture of Engineering Materials & Structures*. 1994; 17(4): 459–467.
13. Donahue RJ, Clark HM, Atanmo P, Kumble R, McEvily AJ. Crack opening displacement and the rate of fatigue crack growth. *International Journal of Fracture Mechanics*. 1972; 8(2): 209–219.

14. Shahani AR, Kashani HM, Rastegar M, Dehkordi MB. A unified model for the fatigue crack growth rate in variable stress ratio. *Fatigue & Fracture of Engineering Materials & Structures*. 2008; 32: 105–118.
15. Gu I, Ritchie RO. On the crack-tip blunting model for fatigue crack propagation in ductile materials. *ASTM Special Technical Publication*. 1999; 1332: 552–564.
16. Tvergaard V. On fatigue crack growth in ductile materials by crack-tip blunting. *Journal of the Mechanics and Physics of Solids*. 2004; 52: 2149–2166.
17. Antunes FV, Rodrigues SM, Branco R, Camas D. A numerical analysis of CTOD in constant amplitude fatigue crack growth. Theoretical and Applied Fracture Mechanics. 2016; 85: 45–55.
18. Chu TC, Ranson WF, Sutton MA, Peters WH. Applications of digital-image correlation technique to experimental mechanics. *Experimental Mechanics*. 1985; 25: 232–244.
19. Sutton MA, Orteu JJ, Schreier HW. *Image Correlation for Shape, Motion and Deformation Measurements: Basic Concepts, Theory and Applications*. New York, USA: Springer Science + Business Media; 2009.
20. Khor W, Moore PL, Pisarki HG, Haslett M, Brown CJ. Measurement and prediction of CTOD in austenitic stainless steel. *Fatigue & Fracture of Engineering Materials & Structures*. 2016; 39: 1433–1442.
21. Schwalbe KH. Introduction of δ_5 as an operational definition of the CTOD and its practical use. ASTM STP 1256. 1995; American Society for Testing and Materials, Philadelphia, PA: 763–778.
22. Samadian K, Hertelé S, De Waele W. Measurement of CTOD along a surface crack by means of digital image correlation. *Engineering Fracture Mechanics*. 2019; 205: 470–485.
23. Ktari A, Baccar M, Shah M, Haddar N, Ayedi HF, Rezai-Aria F. A crack propagation criterion based on ΔCTOD measured with 2D-digital image correlation technique. *Fatigue & Fracture of Engineering Materials & Structures*. 2014; 37(6): 682–694.
24. Korsunsky AM, Song X, Belnoue J, Jun T, Hofmann F, De Matos PFP, Nowell D, Dini D, Aparicio-Blanco O, Walsh MJ. Crack tip deformation fields and fatigue crack growth rates in Ti-6Al-4V. *International Journal of Fatigue*. 2009; 31(11): 1771–1779.
25. Vasco-Olmo JM, James MN, Christopher CJ, Patterson EA, Díaz FA. Assessment of crack tip plastic zone and shape and its influence on crack tip shielding. *Fatigue & Fracture of Engineering Materials & Structures*. 2016; 39: 969–981.

26. Vasco-Olmo JM, Díaz FA, James MN, Yang B. Crack tip plastic zone evolution during an overload cycle and the contribution of plasticity-induced shielding to crack growth rate changes. *Fatigue & Fracture of Engineering Materials & Structures.* 2018; 41: 2172–2186.
27. Yang B, Vasco-Olmo JM, Díaz FA, James MN. A more rationalisation of fatigue crack growth rate data for various specimen geometries and stress ratios using the CJP model. *International Journal of Fatigue*. 2018; 114: 189–197.
28. Christopher CJ, James MN, Patterson EA, Tee KF. Towards a new model of crack tip stress fields. *International Journal of Fracture*. 2007; 148: 361–371.
29. ASTM, E 647 Standard Test Method for Measurement of Fatigue Crack Growth Rates. 2015, American Society for Testing and Materials: Philadelphia, PA.
30. https://www.correlatedsolutions.com/vic-2d/

Table 1 Mechanical properties for the aluminium alloys analysed in the present work

Mechanical property	Unit	Aluminium Alloy	
		2024-T3	7050-T6
Young's modulus, E	GPa	72.3	71.7
Yield stress, σ_{YS}	MPa	348	546
Poisson's ratio, v	-	0.33	0.33

Figures

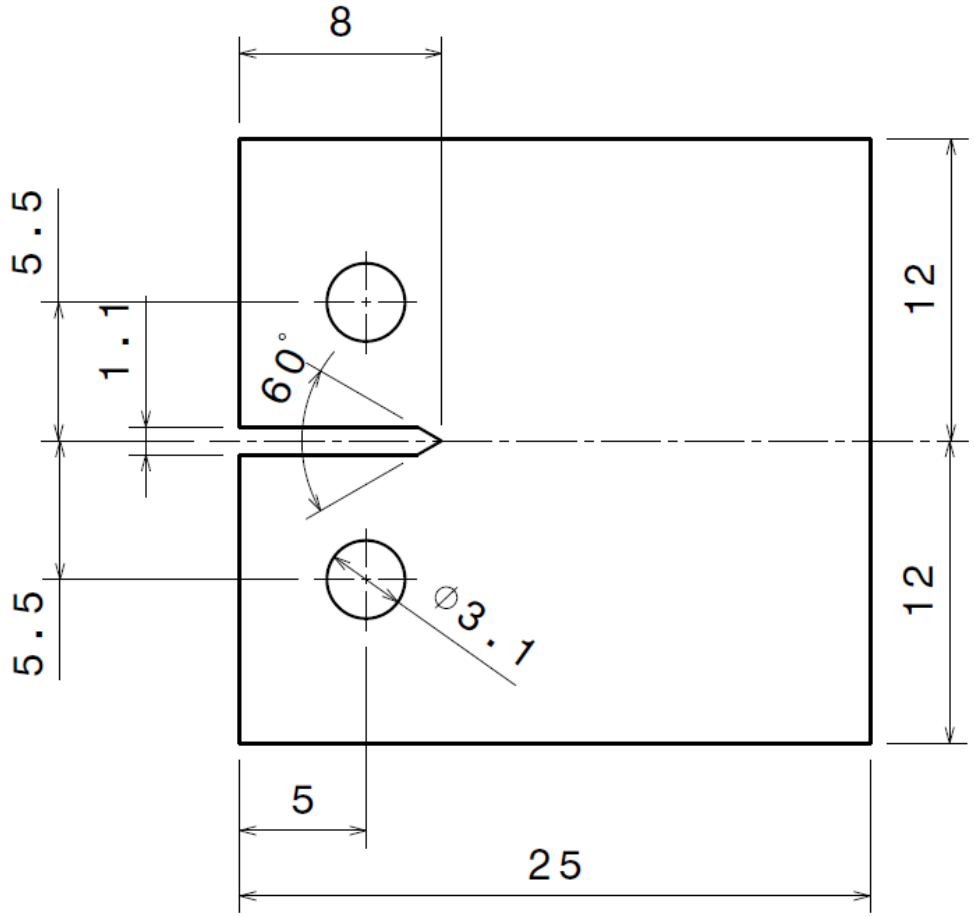

Figure 1 Dimensions (mm) of the CT specimens[29].

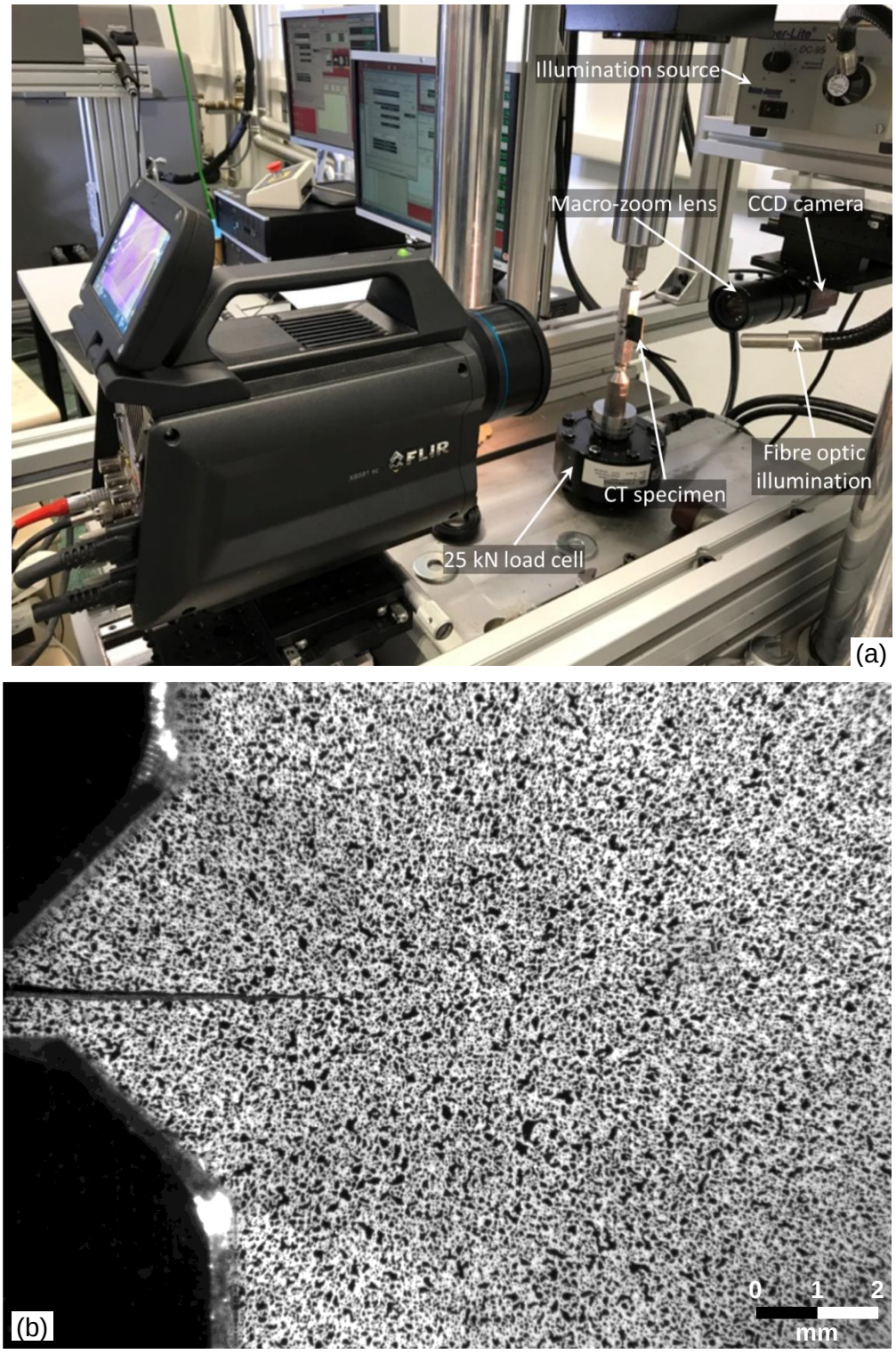

Figure 2 (a) Experimental set-up used in the paper to conduct the fatigue tests and for data acquisition. (b) Image showing the speckle pattern applied on one of the specimen surfaces to implement DIC.

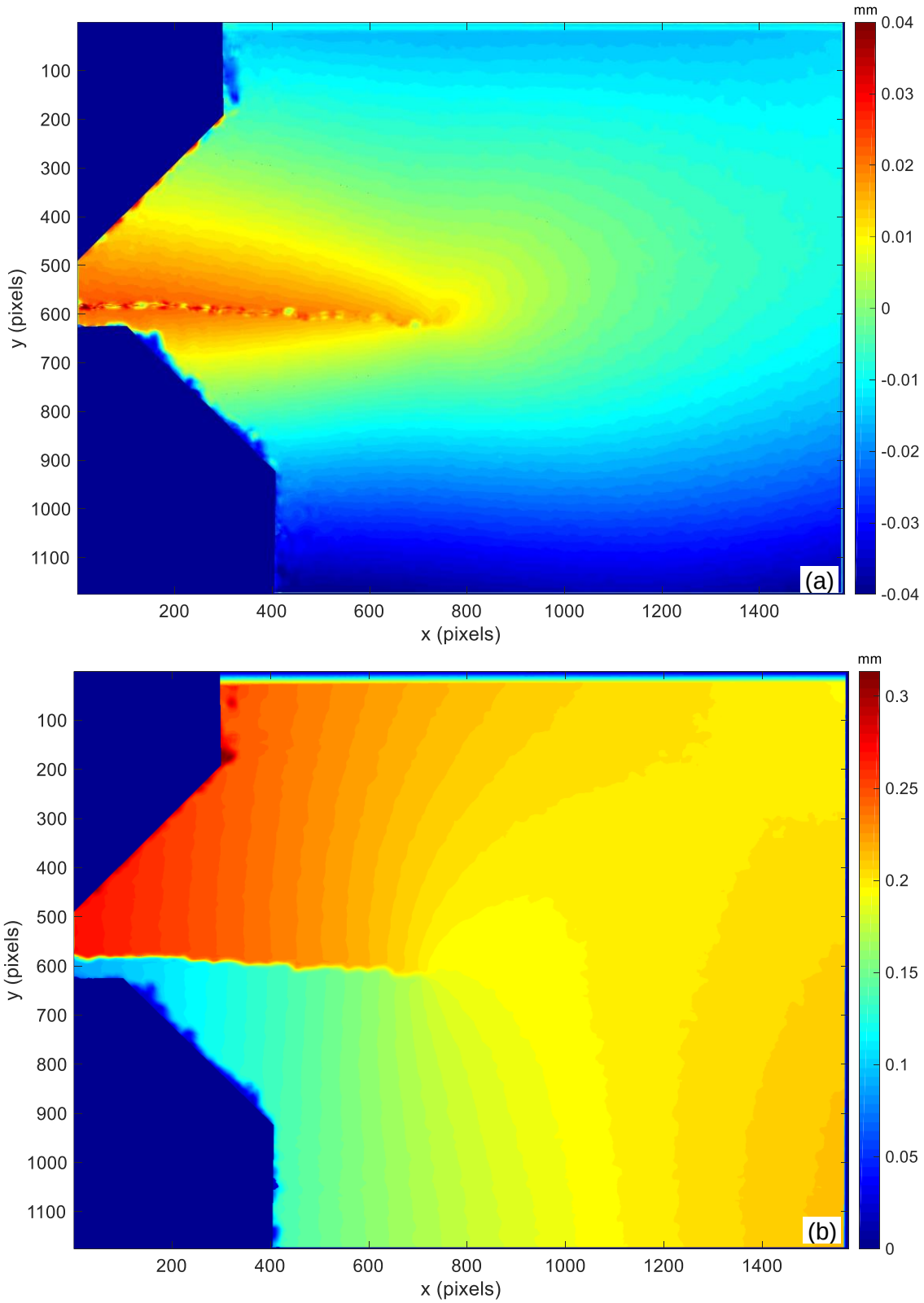

Figure 3 Example of displacement fields obtained by 2D DIC for a load of 600 N and a 9.13 mm crack: Horizontal (a) and vertical (b) displacement maps.

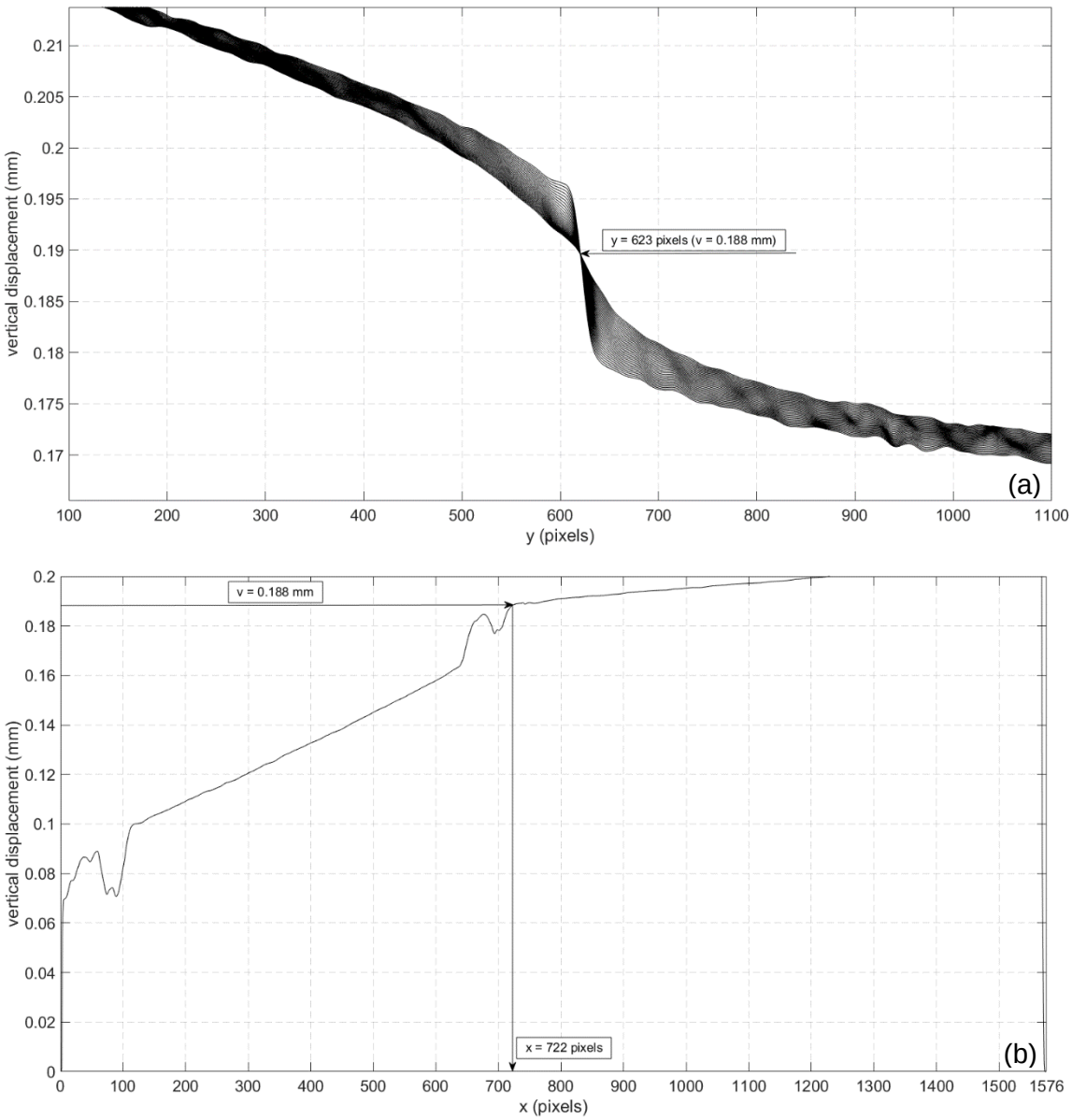

Figure 4 Plots showing the methodology used to identify the position of the crack tip in the *y* (a) and *x* (b) directions.

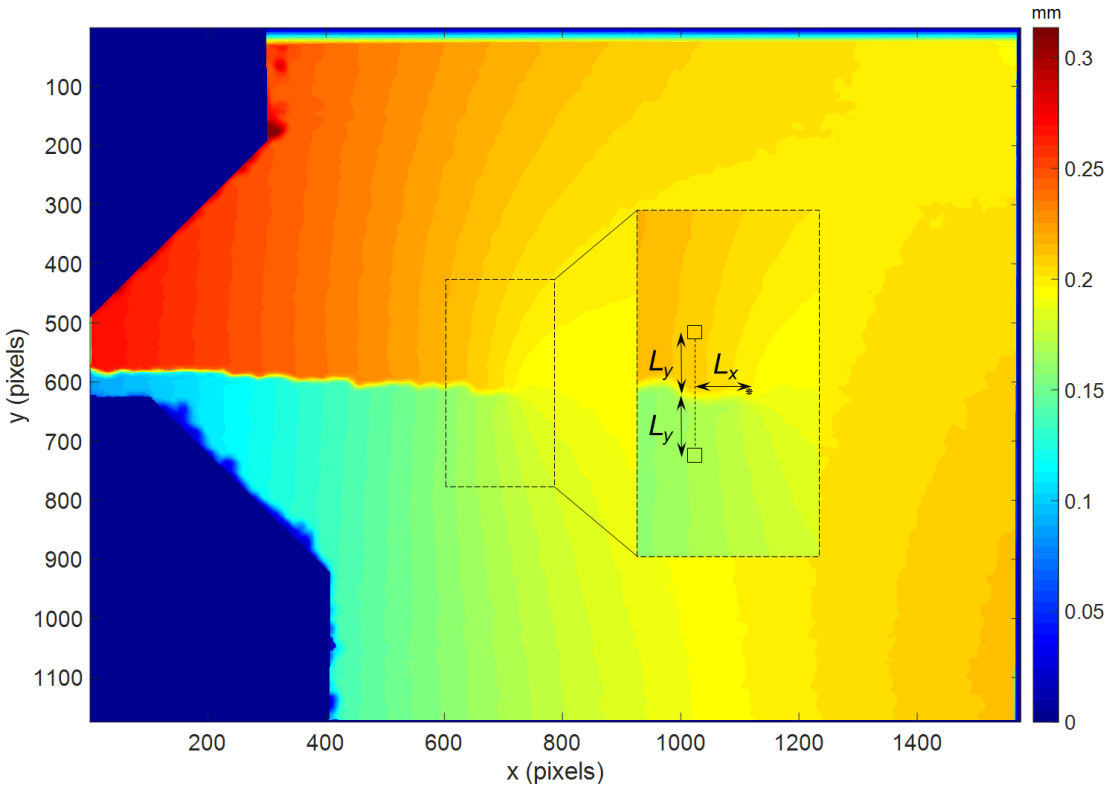

Figure 5 Vertical displacement map with the region around the crack tip enlarged to show the location of the two points used to measure the CTOD. L_x is the horizontal distance behind the crack tip and L_y is the vertical distance from the crack plane.

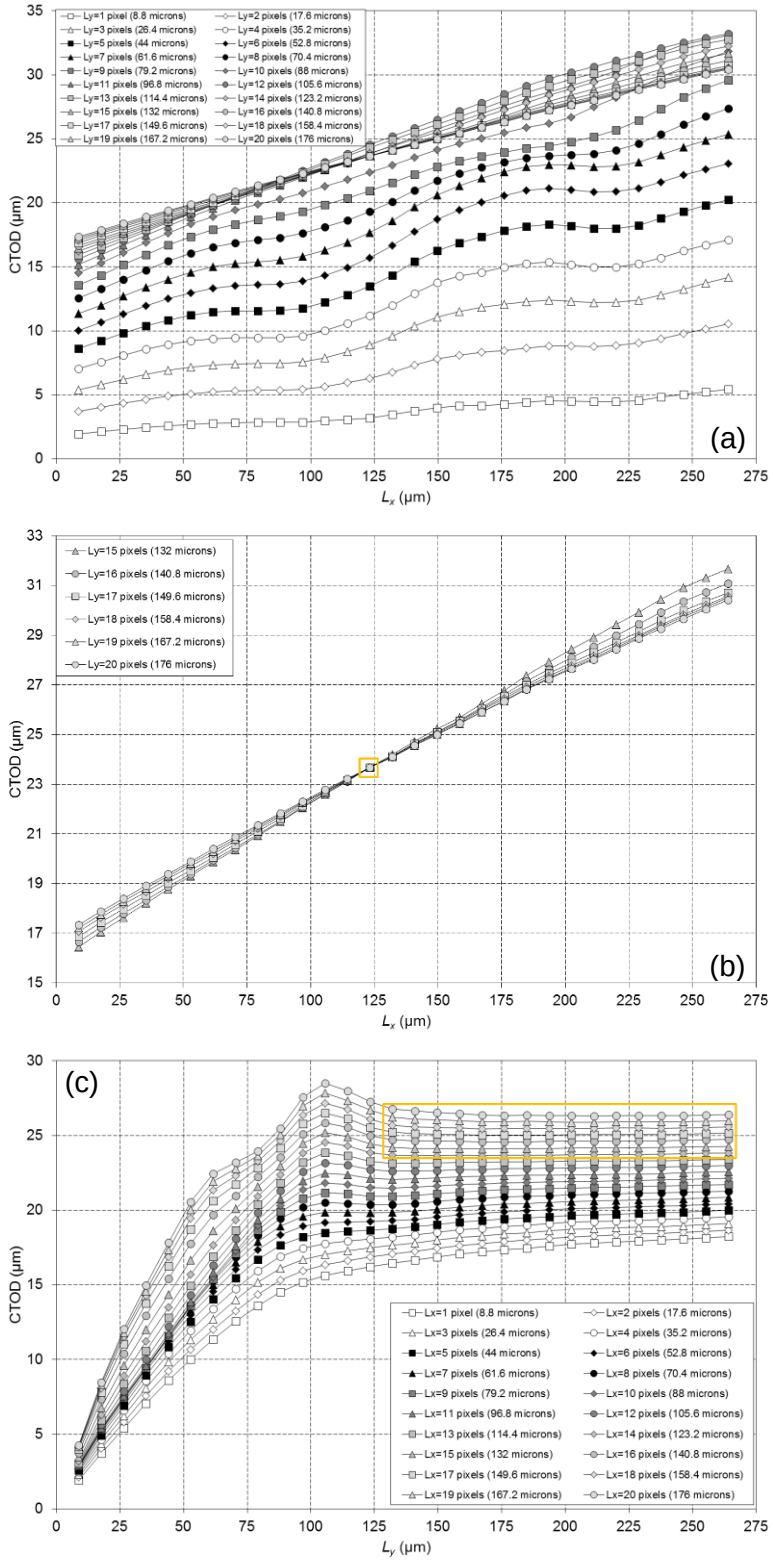

Figure 6 Plots of CTOD showing the effect of the position chosen for the two points where CTOD is measured: (a) Variation of the CTOD values with the distance L_x in the parallel direction to the crack, marking the point where the plots intersect (b); (c) Variation of the CTOD values with the distance L_y in the normal direction to the crack path.

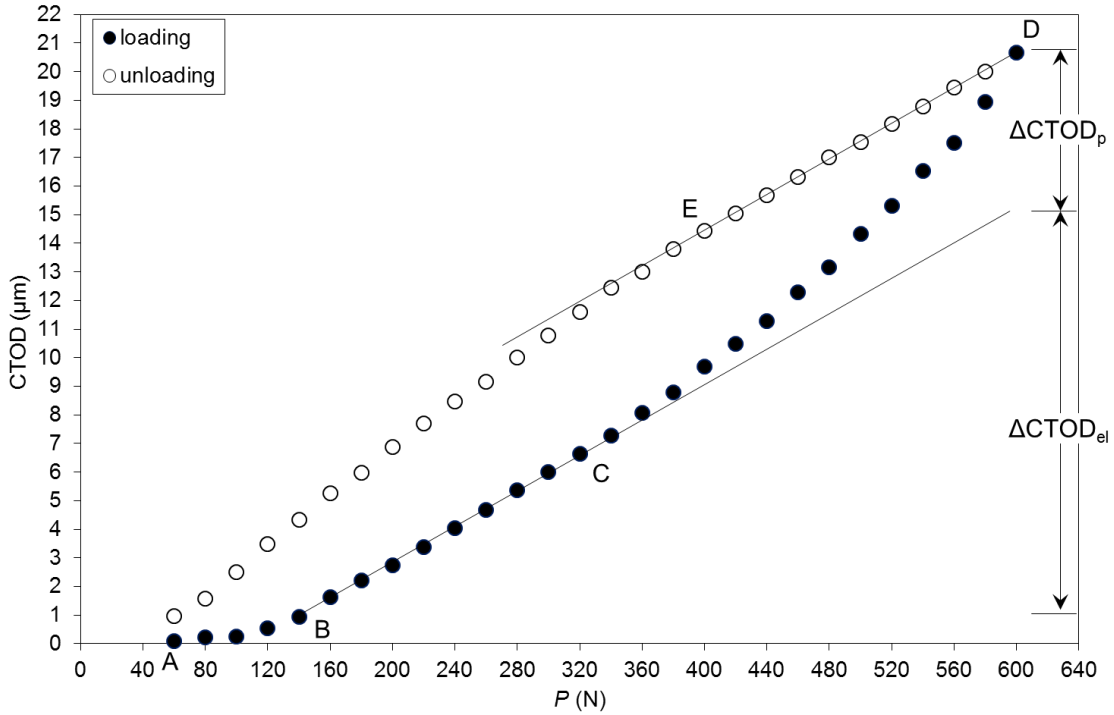

Figure 7 Variation in CTOD throughout a full load cycle for the 7050-T6 aluminium specimen analysed at R = 0.1 and for a 9.13 mm long crack, showing the range of its elastic and plastic components.

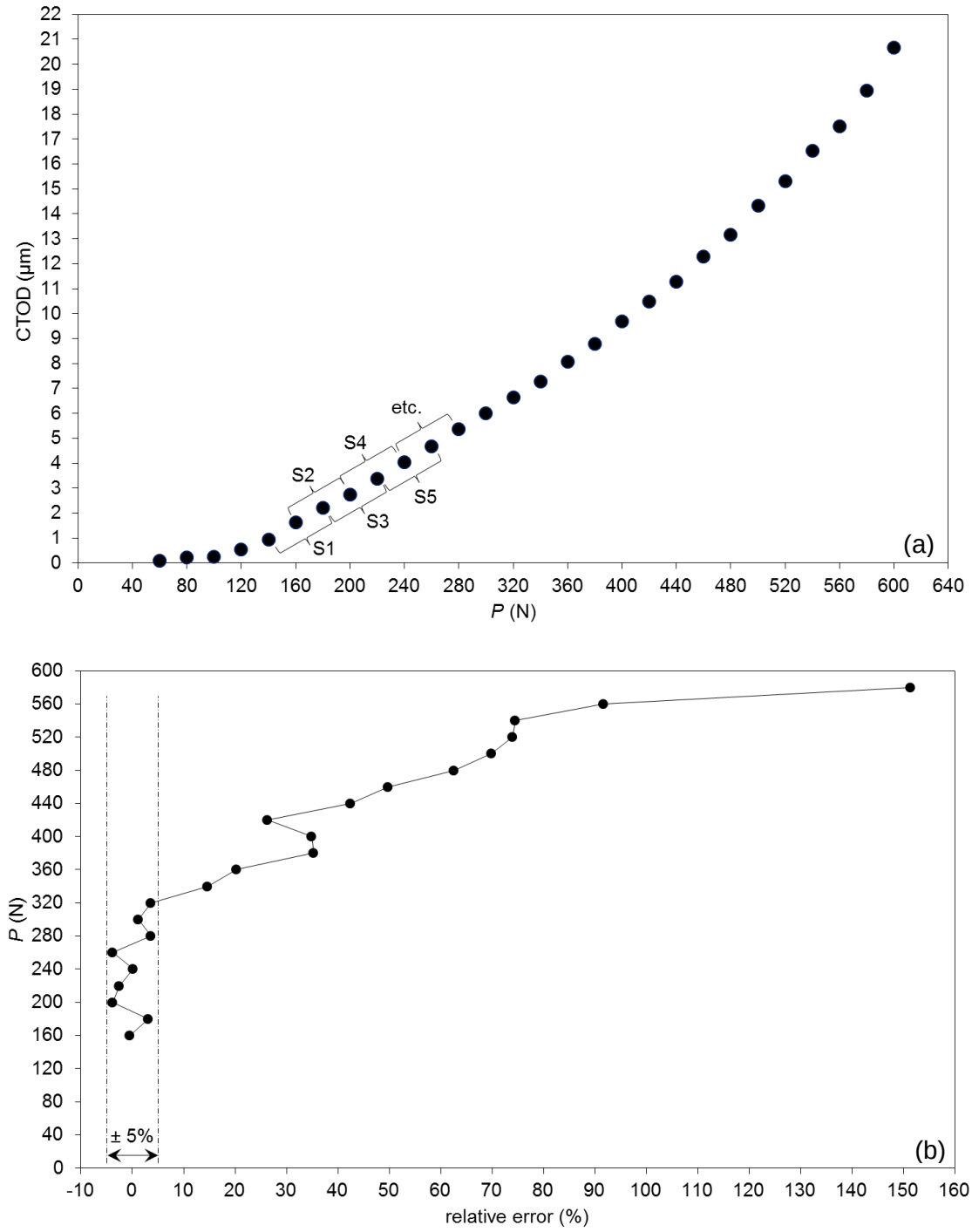

Figure 8 (a) Illustration of the technique used to analyse the CTOD data and determine the ranges of the elastic and plastic CTOD. (b) Variation of the relative error with the applied load. A change in slope of 5% was established as the criterion to identify the end of the region linked to the range of the elastic CTOD.

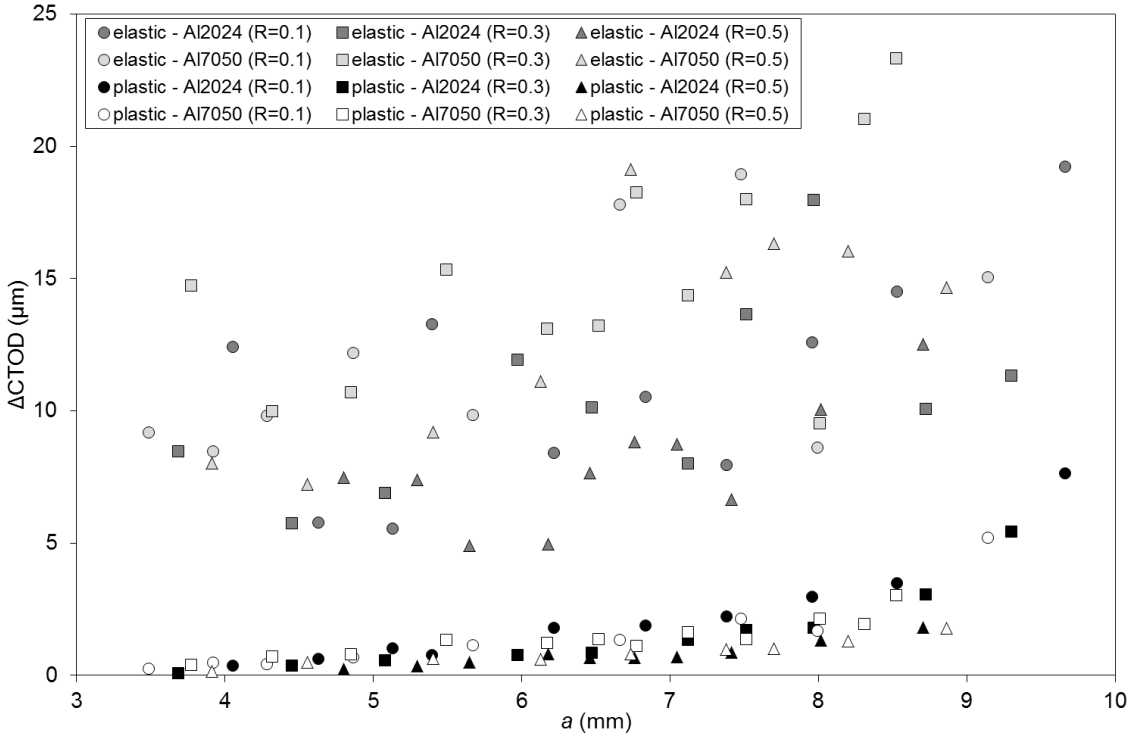

Figure 9 Ranges of elastic and plastic CTOD along the crack length at different stress ratio values for both aluminium alloys.

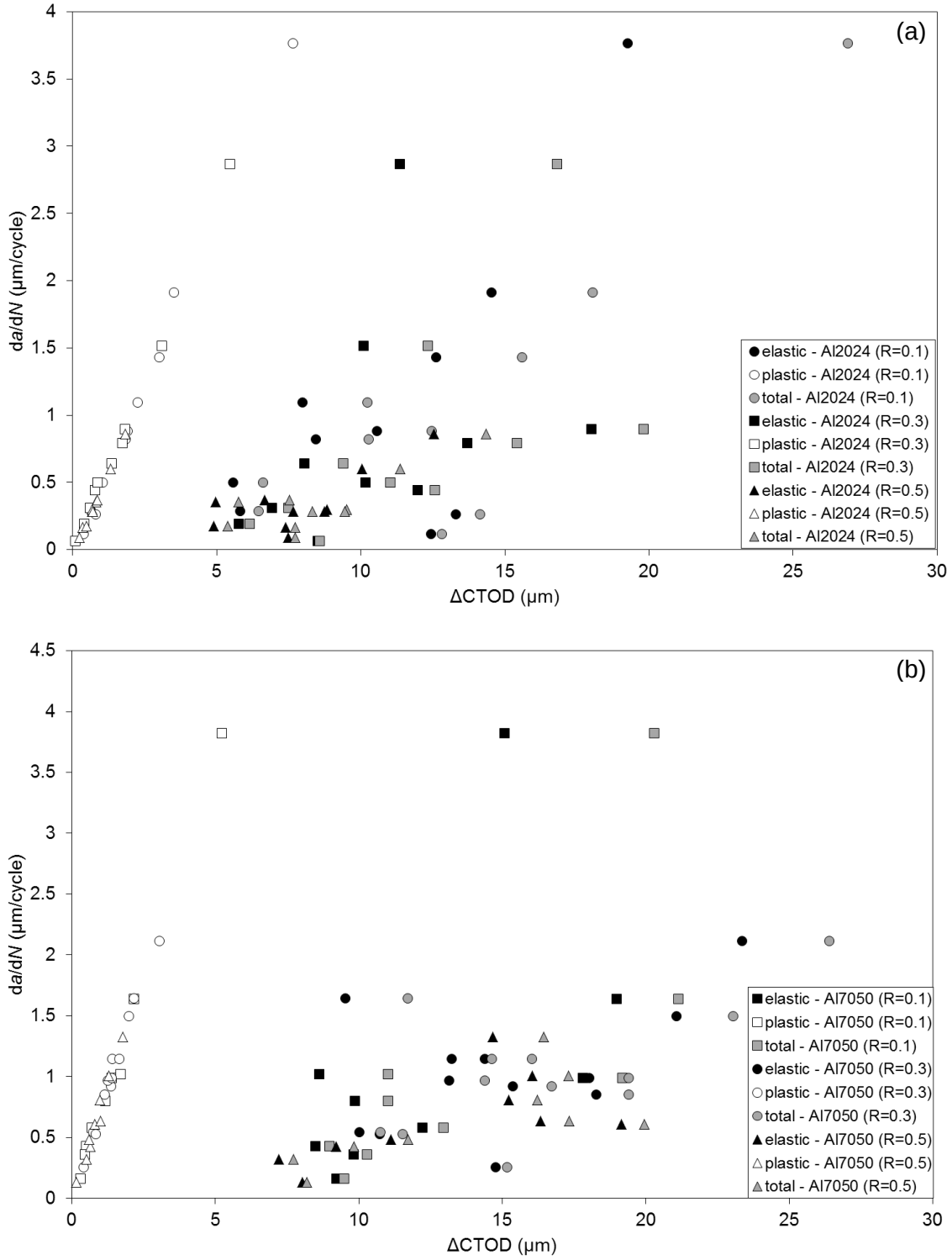

Figure 10 Plots of d*a*/d*N* versus ΔCTOD corresponding to the total, elastic and plastic CTOD for the 2024-T3 (a) and 7050-T6 (b) aluminium alloys.

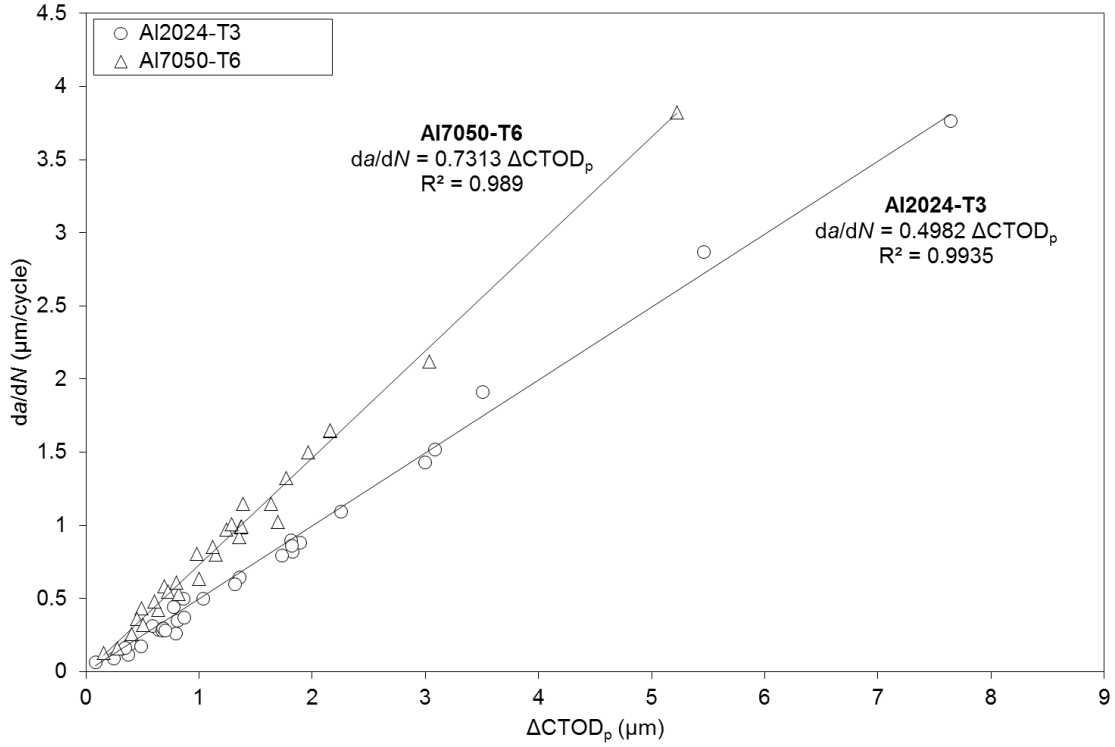

Figure 11 Graph showing the linear variation between d*a*/d*N* and $\Delta CTOD_p$ obtained for both materials.